Pergamon

Journal of Structural Geology, Vol. 19, No. 7, pp. 975 to 986, 1997

0191-8141/97 $17.00 + 0.00

PII: S0191-8141(97)00020-5

Restoration of structural cross-sections

JOHN WICKHAM

Department of Geology, University of Texas at Arlington, Arlington, TX 76019, U.S.A.

and

GEORGE MOECKEL

Mobil Exploration and Producing Technology, 3000 Pegasus Park Drive, Dallas, TX 75247, U.S.A.

(*Received* 13 *May* 1996; *accepted in revised form* 17 *February* 1997)

Abstract—Cross-section restoration transforms deformed stratigraphic boundaries (the cross-section) into a less deformed state at an earlier time in the structural history. It is best described by transformation equations which incorporate rigid translation and rotation plus deformation. These equations can be linear (affine) or non-linear. Strain is a function of the transformation constants, and linear transformation equations produce homogeneous strain. Most existing restorations use linear transformations, and many assume simple shear strain, a special case of linear transformation.

Linear transformations (such as simple shear) cannot, in general, preserve both area and continuity in cross-section restoration: i.e. if area is constrained, there will be gaps and overlaps between different regions of the restored cross-section. If gaps and overlaps are eliminated, area cannot be constrained.

Cross-section restoration can be achieved by solving a geometric boundary value problem using quadrilateral domains with non-linear transformations. The geometric boundary conditions are specified by knowlege of the position of an undeformed layer boundary and the pin line. Strain measured in the field can be incorporated as an initial condition.

Discontinuities (faults) can be incorporated into the solution by treating them as an internal boundary without gaps or overlaps. © 1997 Elsevier Science Ltd.

INTRODUCTION

Cross-section restoration and balancing has its roots in an old method of calculating depth to detachment and shortening (Chamberlain, 1910; Bucher, 1933; Gougel, 1962) which was modified and adapted by Dahlstrom (1969), Mitra and Namson (1989) and others to individual layers in a cross-section. Since then, balanced cross-sections have become widely accepted (Cooper, 1983; Gibbs, 1983; Williams, 1984; Williams and Brooks, 1985; Cooper and Trayner, 1986; Erslev, 1986; Freeth and Ladipo, 1986; Julivert and Arboleya, 1986; De Paor, 1987; Ford, 1987; Cook, 1988; De Paor and Bradley, 1988; Rowan and Kligfield, 1989; Colletta *et al.*, 1990; Mugnier and Rosetti, 1990; Protzman and Mitra, 1990; Searle *et al.*, 1990; McDougall and Hussain, 1991; Nunns, 1991; Sage *et al.*, 1991).

Because of the importance of accurate cross-sections and paleostructure to hydrocarbon exploration, a number of computer programs have been developed which use various methods to restore cross-sections (GEOSEC, Kligfield *et al.*, 1986; LOCACE, Moretti and Larrére, 1989; Triboulet, 1991; BSP, Midland Valley Exploration, Glasgow, U.K.; RESTORE, Texas Bureau of Economic Geology, Austin, Texas, U.S.A.; and proprietary software by petroleum companies).

Much of the interest in cross-section restoration comes from the geometric constraints this process places on geological interpretations. However, an equally important result is the paleostructure shown by the restoration. Paleostructure and its evolution through time relative to hydrocarbon migration can be critical to oil and gas exploration.

Restoration begins with the present deformed state and generates an earlier undeformed (or less deformed) state. Geometric forward modeling (Suppe, 1983; Endignaux and Mugnier, 1990) is the inverse of restoration: it begins with the undeformed state and generates a deformed configuration. Both of these techniques use geometric rules to make their transformations, and neglect any effects due to rheology and forces. Consequently, a geometric restoration or forward model may be formally admissible (Elliott, 1983) but physically impossible.

In the 1970s, concepts of strain and strain measurements in natural structures were applied to the restoration of structural profiles. Oertel (1974) used measurements of strain in a small, single-layered fold to restore it to its original configuration, and Oertel and Ernst (1978) adapted the technique to a multilayered fold by dividing it into domains of homogeneous strain. Schwerdtner (1977) analyzed the restoration of folds using quadrilateral domains and pointed out the problem of strain incompatibility between domains, and the fact that rigid rotation and translation are usually unknown. Hossack (1978) used integration along strain trajectories

to restore layers to their original thickness, and Cobbold (1979) introduced a method using 'finite elements' (similar to Schwerdtner's domains and not to be confused with the numerical method of solving dynamic equations) and strain trajectories to restore deformed structures. Cobbold and Percevault (1983) showed that the 'finite element' method can be treated as an Euler integration of displacement gradients but, for the general case, strain incompatibilities between elements would always exist. They devised a least-squares method to minimize these incompatibilities. Woodward *et al.* (1986) combined the 'finite element' and strain integration methods with the older cross-section balancing techniques so that deformation with ductile flow could be included in balanced cross-sections.

By the end of the 1980s, strain data could be used to approximately restore structures using finite elements or domains. Strain was assumed to be homogeneous within each domain, there were little or no data on rigid-body rotations, and gaps, overlaps and strain incompatibilities between adjacent domains remained a significant problem. De Paor (1990) devised a special non-linear transformation matrix which kept the edges of quadrilateral domains straight and eliminated gaps and overlaps. However, the elimination of these incompatibilities resulted in an unspecified area strain.

Howard (1993) pointed out that strain data could be converted into transformation (or displacement) functions at the strain data points. These displacement functions could then be interpolated graphically between data points giving non-linear functions which could be used to restore a layer without generating gaps, overlaps or strain incompatibilities between domains.

Another interesting approach to restoration, which is applicable to cross-sections in which the pathline (or streakline) of a material element can be inferred during deformation, was described by Morgan *et al.* (1994) and Morgan and Karig (1995). This method involves the solution of the Lagrangian form of the conservation of mass equation within deforming domains, and was applied to the toe of a deforming accretionary prism. This technique requires information on volume/density changes and some simplifying assumptions not normally available from paleostructures.

Both restoration and geometric forward modeling are problems in analytical geometry which can be described mathematically by geometric transformations and finite strain. The purpose of this paper is to analyze the restoration process from an analytical geometry point of view, and to show how cross-sections with faults can be restored by solving a geometric boundary value problem.

GEOMETRIC TRANSFORMATIONS

In forward modeling, the co-ordinates of the deformed configuration (x) are given as a function of the undeformed co-ordinates (X) in a Lagrangian reference frame (Means, 1976; Ramsay and Huber, 1983). An Eulerian description is used in restoration in which the undeformed co-ordinates (X) are given as a function of the deformed position (x). This is the framework used here. In two dimensions, for example, the Eulerian transformation equations over some domain can be approximated by:

$$\begin{aligned} X_1 &= D_{10} + D_{11}x_1 + D_{12}x_2 + D_{13}x_1^2 + D_{14}x_1x_2 + D_{15}x_2^2 \\ X_2 &= D_{20} + D_{21}x_1 + D_{22}x_2 + D_{23}x_1^2 + D_{24}x_1x_2 + D_{25}x_2^2, \end{aligned} \tag{1}$$

where D_{ij} are the transformation constants. These equations are written only to the second order, in part for simplicity but also because solutions to higher-order equations require more information than is usually available from cross-sections. However, it is easy to extend the equations to higher orders.

The discussion in this paper is limited to two dimensions. While this has been the assumption in all cross-section restoration, it limits the application to plane strain. Plane strain is rare in nature, so cross-section restoration should always be considered an approximation whose reliability depends on the degree to which plane-strain deformation has occurred. An extension of this approach to three dimensions is currently being developed.

The Eulerian deformation gradients (Means, 1976) are:

$$\begin{aligned} \partial X_1/\partial x_1 &= D_{11} + 2D_{13}x_1 + D_{14}x_2 \\ \partial X_1/\partial x_2 &= D_{12} + D_{14}x_1 + 2D_{15}x_2 \\ \partial X_2/\partial x_1 &= D_{21} + 2D_{23}x_1 + D_{24}x_2 \\ \partial X_2/\partial x_2 &= D_{22} + D_{24}x_1 + 2D_{25}x_2 \end{aligned} \tag{2}$$

and the Cauchy strain tensor (using tensor notation) is

$$c_{ij} = \partial X_k/\partial x_i \; \partial X_k/\partial x_j \tag{3}$$

and

$$\begin{aligned} c_{11} = &(D_{11})^2 + (D_{21})^2 + 4(D_{11}D_{13} + D_{21}D_{23})x_1 + \\ &2(D_{11}D_{14} + D_{23}D_{24})x_2 + 4(D_{13})^2 + (D_{23})^2x_1^2 + \\ &4(D_{13}D_{14} + D_{23}D_{24})x_1x_2 + (D_{14})^2 + (D_{24})^2x_2^2 \end{aligned} \tag{4}$$

Note that the deformation gradients (equation (2) and strain (equation (3) are functions of position within the domain because the transformation equations are non-linear. If they were linear (affine) the gradients and the strain would be constant (homogeneous) over the domain.

TRANSFORMATION EQUATIONS IN CROSS-SECTION RESTORATION

The geometric boundary value process of reconstructing cross-sections consists of dividing the cross-section

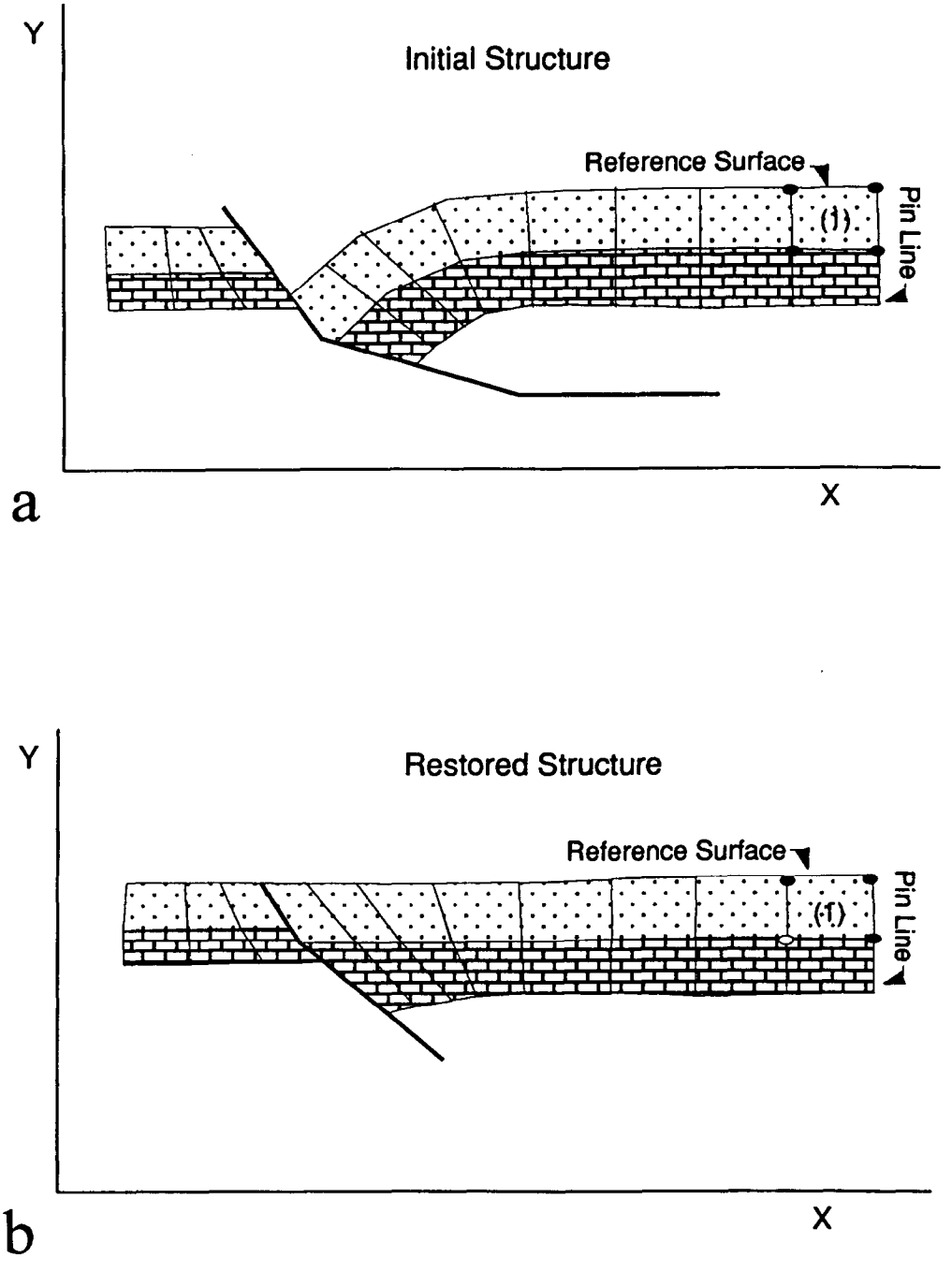

Fig. 1. Restoration of roll-over using quadrilateral domains. (a) The initial configuration with the top boundary as the reference surface and the right edge as the pin line. The black dots mark the known co-ordinates of the corner of domain 1. (b) The restored cross-section with the reference boundary horizontal. The three black dots represent known co-ordinates in the restored cross-section because they are on the reference boundary and the pin line. This produces six equations (x, y for each dot) relating the restored co-ordinate to the initial co-ordinate. These six equations must be used to find the transformation constants to calculate the location of the unknown corner of the quadrilateral (white dot).

into domains (Fig. 1a), and then restoring each domain successively by translation, rotation and strain so that they all fit together in an undeformed configuration (Fig. 1b). Quadrilateral domains seem to be the most efficient for this purpose.

The restoration of each domain is described by an Eulerian transformation equation. For example, domain 1 (Fig. 1a) is bounded by the reference surface and the pin line. The pin line and reference surface are presumed to be known in the undeformed state (Fig. 1b), and the co-ordinates of these two surfaces become the boundary conditions of the geometric problem. For example, in the deformed state the co-ordinates of all four corners of domain 1 (Fig. 1a) are known, and in the undeformed state three corners are known, the ones along the reference surface and pin line (Fig. 1b).

To restore domain 1 and determine the co-ordinates of its fourth corner in the undeformed state, it is necessary to solve for transformation constants in equations similar to equation (1). Once those constants are known, the undeformed position of the fourth corner (as well as all other points within the domain) can be calculated.

It is possible to set up a number of equations involving the transformation constants in order to find solutions for the constants. (Because the number of transformation constants must equal the number of equations, the form of the transformation equations is limited.) In two dimensions, there are six equations for the three corners on the external boundary of quadrilateral domain 1 (Fig. 1).

Presumably, linear transformation equations could be used because they have only six constants:

$$\begin{aligned} X_1 &= D_{10} + D_{11}x_1 + D_{12}x_2 \\ X_2 &= D_{20} + D_{21}x_1 + D_{22}x_2. \end{aligned} \tag{5}$$

However, if area is constrained, at least one additional equation must be added, so the six constants of equation (5) are not enough. This is an example of the generalization that affine (linear) transformations cannot constrain area of restored domains without creating gaps and overlaps between adjacent domains. If six linear equations are constructed that do constrain area (by reducing the number of corners used), then adjacent domains will have gaps or overlaps in the restored section. Layer-parallel simple shear is a special case where both area and continuity can be preserved, but only if the upper and lower boundaries of the layer are parallel.

The only transformation that can both constrain area and preserve continuity is non-linear. One possible equation for quadrilateral domains is:

$$\begin{aligned} X_1 &= D_{10} + D_{11}x_1 + D_{12}x_2 + D_{13}f(x_i, x_j) \\ X_2 &= D_{20} + D_{21}x_1 + D_{22}x_2 + D_{23}g(x_i, x_j), \end{aligned} \tag{6}$$

where $f(x_i, x_j)$ and $g(x_i, x_j)$ are some convenient functions of the unrestored co-ordinates.

In general, when transformations of the type described by equation (6) are applied to quadrilateral domains, the four straight lines

$$l_m(x_i, x_j) = a_m x_1 + b_m x_2 + c_m = 0 \ (m = 1, 2, 3, 4) \tag{7}$$

forming the edges of the initial quadrilateral domain will transform into a curvilinear quadrilateral in the restored configuration. In a restored cross-section consisting of a large number of quadrilaterals, the curved edges of adjacent quadrilaterals may not coincide resulting in gaps or overlaps. However, $f(x_i, x_j)$ and $g(x_i, x_j)$ (equation (6) may be chosen so that the boundaries of quadrilaterals remain straight lines after transformation. For example, De Paor (1990) chose a non-linear transformation in which lines parallel to the co-ordinate system remain linear after the transformation so that variables in equation (6) are:

$$\begin{aligned} f(x_i, x_j) = g(x_i, x_j) &= x_1 x_2 \\ D_{13} &= D_{11}\delta x_1 + D_{12}\delta x_2 \\ D_{23} &= D_{21}\delta x_1 + D_{22}\delta x_2 \end{aligned} \tag{8}$$

where δx_i are constants (De Paor, 1990).

Alternatively, $f(x_i, x_j)$ and $g(x_i, x_j)$ in equation (6) can be chosen such that the evaluations $f(l_m) = g(l_m) = 0$. In that case, adjacent domains in the restored cross-section have compatible, non-overlapping boundaries. This choice is always possible from the class of all non-linear functions of the plane variables x and y. For example, the non-linear function,

$$h(x_i, x_j) = \prod_{m=1}^{4} l_m(x_i, x_j), \tag{9}$$

defined for points in the interior and on the boundary of any quadrilateral domain of the unrestored section, obtains values $h(l_m) = 0$ on all sides of the quadrilateral. Using $h(x_i, x_j)$ (equation (9) for both $f(x_i, x_j)$ and $g(x_i, x_j)$ in equation (6), these non-linear functions $f(x_i, x_j)$ and $g(x_i, x_j)$ take on linear function forms on the boundaries l_m of a quadrilateral domain in the unrestored configuration. Numerical constants a_m, b_m and c_m (equation (7) are prescribed so that $h(x_i, x_j) = f(x_i, x_j) = g(x_i, x_j)$ are continuous on the boundaries of the quadrilateral. The transformation equation to be solved is:

$$\begin{aligned} X_1 &= D_{10} + D_{11}x_1 + D_{12}x_2 + D_{13}\left\{\prod_{m=1}^{4} l_m(x_i, x_j)\right\} \\ X_2 &= D_{20} + D_{21}x_1 + D_{22}x_2 + D_{23}\left\{\prod_{m=1}^{4} l_m(x_i, x_j)\right\} \end{aligned} \tag{10}$$

where $l_m(x_i, x_j)$ is from equation (7)

This functional form has eight transformation constants, and quadrilateral domains with straight edges in the unrestored configuration are transformed into non-overlapping quadrilaterals with straight edges in the restored configuration. However, information from the three known corners of the quadrilateral domain only provides six equations, so two additional equations are required to solve for all eight constants.

It is essential to constrain the area of each quadrilateral domain in some sense. A deformation is said to be isochoric if the Jacobian $(D) = 1$. This pointwise isochoric condition will assure the preservation of area during transformation of quadrilateral domains. However, this is difficult to impose in practice. One way to add two additional area constraints to find all eight constants is to divide the quadrilateral domain into two triangles and to constrain the area of each triangle. For a constant area transformation

$$a_1(x_i, x_j) = \zeta_1 A_1(X_i, X_j) \text{ and } a_2(x_i, x_j) = \zeta_2 A_2(X_i, X_j), \tag{11}$$

where a_1 and a_2 are areas of the two triangles in the

unrestored domain, A_1 and A_2 are the areas of the same triangles in the restored domain, and ζ_1 and ζ_2 represent the area change during the restoration. Both of these area constraints can be written in terms of the transformation constants. The six equations derived from the three quadrilateral corners and the two area constraints are eight equations which can be solved for the eight unknown transformation constants in equation (10).

USE OF NATURAL STRAIN DATA IN RESTORATION

Measurements of strain along the cross-section may be available (Woodward *et al.*, 1986), and can be included in the cross-section restoration boundary value problem. Strain data are commonly given in terms of the magnitude and orientation of the principal directions, and we will use quadratic elongation (λ) and orientation (θ') measured in the Eulerian reference frame. Unfortunately, the rigid rotation component (ω) can seldom be estimated, so it will not be used as a constraint in the boundary value problem.

Strain is defined at a material point and is a function of the deformation gradients (or displacement gradients) evaluated at that point. Ramsay and Huber (1983, appendix C) have derived the Lagrangian equations relating deformation gradients to strain and rotation. The eqivalent Eulerian relationships are:

$$\begin{aligned}
\partial X_1/\partial x_1 &= \cos\omega(\lambda_1 \sin^2\theta' + \lambda_2 \cos^2\theta')/\lambda_1\lambda_2 \\
&\quad + \sin\omega \sin\theta' \cos\theta'(\lambda_2 - \lambda_1)/\lambda_1\lambda_2 \\
\partial X_2/\partial x_1 &= \cos\omega \sin\theta' \cos\theta'(\lambda_2 - \lambda_1)/\lambda_1\lambda_2 \\
&\quad + \sin\omega(\lambda_2 \sin^2\theta' + \lambda_1 \cos^2\theta')/\lambda_1\lambda_2 \\
\partial X_1/\partial x_2 &= \cos\omega \sin\theta' \cos\theta'(\lambda_2 - \lambda_1)/\lambda_1\lambda_2 \\
&\quad - \sin\omega(\lambda_1 \sin^2\theta' + \lambda_2 \cos^2\theta')/\lambda_1\lambda_2 \\
\partial X_2/\partial x_2 &= \cos\omega(\lambda_2 \sin^2\theta' + \lambda_1 \cos^2\theta')/\lambda_1\lambda_2 \\
&\quad - \sin\omega \sin\theta' \cos\theta'(\lambda_2 - \lambda_1)/\lambda_1\lambda_2
\end{aligned} \tag{12}$$

Eliminating ω (by subtracting the 3rd from the 2nd, and adding the 1st and 4th of equation (12) leaves two independent equations relating the strain parameters to the deformation gradients:

$$\begin{aligned}
0 &= -(\lambda_1 \cos^2\theta' + \lambda_2 \sin^2\theta')\partial X_1/\partial x_1 + \sin\theta' \cos\theta' \\
&\quad (\lambda_2 - \lambda_1)\partial X_2/\partial x_1 - \sin\theta' \cos\theta'(\lambda_2 - \lambda_1)\partial X_1/\partial x_2 \\
&\quad + (\lambda_1 \sin^2\theta' + \lambda_2 \cos^2\theta')\partial X_2/\partial x_2 \\
0 &= \sin\theta' \cos\theta'(\lambda_2 - \lambda_1)\partial X_1/\partial x_1 - (\lambda_1 \sin^2\theta' \\
&\quad + \lambda_2 \cos^2\theta')\partial X_2/\partial x_1 - (\lambda_1 \cos^2\theta' + \lambda_2 \sin^2\theta') \\
&\quad \partial X_1/\partial x_2 + \sin\theta' \cos\theta'(\lambda_2 - \lambda_1)\partial X_2/\partial x_2.
\end{aligned} \tag{13}$$

However, the deformation gradients in equations (12) and (13) are functions of the transformation constants in equation (6):

$$\begin{aligned}
\partial X_1/\partial x_1 &= D_{11} + D_{13}\partial f(x_i, x_j)/\partial x_1 \\
\partial X_2/\partial x_1 &= D_{21} + D_{23}\partial g(x_i, x_j)/\partial x_1 \\
\partial X_1/\partial x_2 &= D_{12} + D_{13}\partial f(x_i, x_j)/\partial x_2 \\
\partial X_2/\partial x_2 &= D_{22} + D_{23}\partial g(x_i, x_j)/\partial x_2
\end{aligned} \tag{14}$$

Substituting equation (14) into equation (13) provides two independent equations relating strain parameters to the transformation constants of non-linear transformation equations:

$$\begin{aligned}
0 &= -(\lambda_1 \cos^2\theta' + \lambda_2 \sin^2\theta')D_{11} - \sin\theta' \cos\theta' \\
&\quad (\lambda_2 - \lambda_1)D_{12} - \{(\lambda_1 \cos^2\theta' + \lambda_2 \sin^2\theta') \\
&\quad \partial f(x_i, x_j)/\partial x_1 + \sin\theta' \cos\theta'(\lambda_2 - \lambda_1)\partial f(x_i, x_j)/\partial x_2\} \\
&\quad D_{13} + \sin\theta' \cos\theta'(\lambda_2 - \lambda_1)D_{21} + (\lambda_1 \sin^2\theta' + \lambda_2 \\
&\quad \cos^2\theta')D_{22} + \{(\lambda_1 \sin^2\theta' + \lambda_2 \cos^2\theta')\partial g(x_i, x_j)/\partial x_2 \\
&\quad + \sin\theta' \cos\theta'(\lambda_2 - \lambda_1)\partial g(x_i, x_j)/\partial x_1\}D_{23}
\end{aligned} \tag{15a}$$

$$\begin{aligned}
0 &= \sin\theta' \cos\theta'(\lambda_2 - \lambda_1)D_{11} - (\lambda_1 \cos^2\theta' + \lambda_2 \sin^2\theta')D_{12} \\
&\quad - \{(\lambda_1 \cos^2\theta' + \lambda_2 \sin^2\theta')\partial f(x_i, x_j)/\partial x_2 - \sin\theta' \\
&\quad \cos\theta'(\lambda_2 - \lambda_1)\partial f(x_i, x_j)/\partial x_1\}D_{13} - (\lambda_1 \sin^2\theta' + \lambda_2 \\
&\quad \cos^2\theta')D_{21} + \sin\theta' \cos\theta'(\lambda_2 - \lambda_1)D_{22} + \{\sin\theta' \cos\theta' \\
&\quad (\lambda_2 - \lambda_1)\partial g(x_i, x_j)/\partial x_2 - (\lambda_1 \sin^2\theta' + \lambda_2 \cos^2\theta') \\
&\quad \partial g(x_i, x_j)/\partial x_1\}D_{23}.
\end{aligned} \tag{15b}$$

Equations (15a) and (15b) apply to a material point at which the strain has been measured. So in principle, there would be a set of two equations available for each point in the domain where the strain parameters had been measured.

The non-linear transformation equations (equation (10) have eight transformation constants to be determined in a quadrilateral domain. Six of those equations come from three known corners of the domain, and the other two can be obtained from area constraints. If strain data are available, then two more equations (equations (15a) and (15b)) for each strain data point within the domain can be obtained, so the problem becomes over-constrained. If strain data are available, there is an easy way to add more transformation constants to equation (10). The function

$$\prod_{m=1}^{4} l_m(x_i, x_j) \tag{16}$$

in equation (10) has 15 terms with only one transformation constant. So it would be possible to add up to 12 additional transformation constants to accommodate up to six strain data points within a domain.

CONSTRAINTS ACROSS FAULTS

It is possible to reconstruct the first fault block, domain by domain, to its undeformed configuration knowing the undeformed co-ordinates of the points along the top layer (flat or a known topography) and a pin line (Fig. 1). The next fault block must fit against the undeformed fault of the first block, and the fault becomes the 'pin' line for the second fault block (Fig. 1b). Again, the undeformed co-ordinates of the top of the second fault block are assumed known. If there is a thickness change across this fault, the stratigraphic boundaries of one fault block will not match equivalent boundaries in the adjacent fault block in the undeformed configuration. In other words, the fault could be a discontinuity in both the deformed and undeformed state.

Constraints on deformation at fault boundaries can be derived from the geometric consequences of smoothness, and non-linear analysis is essential to establish required boundary conditions at faults. The relationships we have derived (Appendix I) are based on two geometric necessities: (1) there can be no gaps or overlaps between adjacent fault blocks; and (2) the deformation on one side of the fault is related to the deformation on the other side of the fault, the fault curvatures in the deformed and undeformed state, and the amount of displacement along the fault (see equation (A20) of Appendix I).

In the restoration procedure outlined in Appendix I, the curvature of both the deformed and undeformed fault, the strain distribution on one side of the fault, and fault slip can all be calculated or estimated. From this information, strains and displacements on the other side of the fault can be calculated to get the undeformed configuration of the adjacent fault block.

Employing the two-dimensional, plane-strain assumption used here, slip on faults must be confined to the plane of the cross-section to make the restoration. A fully three-dimensional treatment of restoration (under development) is necessary to adequately account for oblique or strike-slip movement along faults.

BOUNDARY CONDITIONS AND LINEAR MODELS

Any restoration method must make some assumptions about the undeformed configuration (boundary conditions) and the transformation model. Most assume that the uppermost layer was initially horizontal, and that one edge (the pin line) has the same orientation in the undeformed as it has in the deformed configuration.

The restoration is very sensitive to the choice of boundary conditions (see Geiser *et al.*, 1988 for a discussion of the effect of pin lines). If the boundary conditions are not geologically accurate, the restoration will not be reliable no matter how good the cross-section looks.

The constraint of working in two dimensions (plane strain) is also problematic. In nature, fault displacements seldom occur in the plane of the cross-section, and there is commonly a component of strain perpendicular to the cross-section. If these violations of plane strain are significant, then two-dimensional restoration is not reliable.

In addition to the pin line, the topography or bathymetry of the top boundary must also be specified in the restored section. Most assume that this layer was flat and horizontal because its initial shape usually cannot be known with certainty. However, the shape of the top boundary can affect the restored section as dramatically as the pin line, and errors in the shape of the top boundary will produce errors in the reconstruction.

Most restoration and balancing methods assume a linear transformation model. For example, layer-parallel simple shear assumes that layer boundary length in the restored section is the same as it is in the unrestored section and that there are no tectonically induced thickness changes either. Simple shear inclined to layering always introduces changes in layer length and thickness which depend on the inclination. Consequently, the configuration of the restored section is also dependent on the linear transformation chosen. A linear transformation is so restrictive that it cannot even preserve continuity between adjacent domains, so it will distort the restored section unless the natural deformation followed the same linear transformation, which is very unlikely. Non-linear transformations are the only ones that can portray the complexity of natural deformation, yet also be capable of duplicating the simpler linear transformations.

EXAMPLES OF CROSS-SECTION RESTORATIONS

A UNIX-based computer program has been written using much of the non-linear approach outlined here. Figure 2 is an example of a cross-section that has been restored using non-linear transformations and quadrilateral domains. The major advantages of this approach are as follows.

(1) Control of both area and continuity is assured for inhomogeneous geological deformation (which is the rule rather than the exception).

(2) Dividing each layer of the cross-section into quadrilateral domains means that the restoration can be done layer by layer within a fault block rather than being forced to restore the whole fault block at once. Thickness variations within each layer can be properly restored (Fig. 2). In addition, both synthetic and antithetic faults can be restored which is a serious problem for some programs using simple shear with faults as pin lines.

(3) The finite strain, rigid rotation and translation can

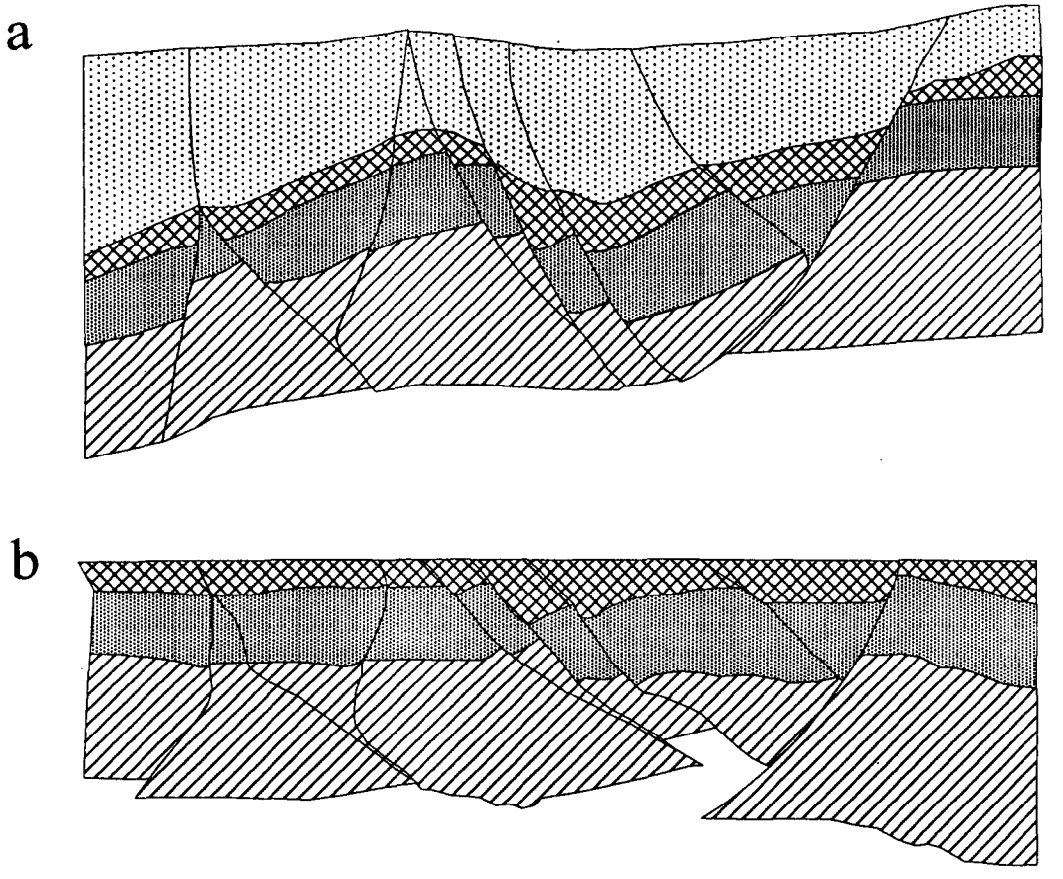

Fig. 2. (a) A cross-section from an interpreted seismic line from the North Sea. (b) A restoration on top of the second layer based on a non-linear transformation of quadrilateral domains. The right-hand side of the cross-section is a pin line. Note that intersecting faults can be restored. The gap in the lowest layer suggests that the interpretation may be erroneous or that movement of material out of the plane of the cross-section has occurred.

be calculated within each domain. This represents the strain required to transform the cross-section from its deformed to undeformed configuration. The reciprocal of that strain represents the deformation that has accumulated in the deformed cross-section, and can be used as a further constraint on the reliability of the cross-section. If the local strain in a domain is extremely different from that observed in the rocks, there is something wrong with the cross-section, its assumed boundary constraints or the transformation model.

(4) Finally, because total strain can be calculated, quantitative constraints can be imposed to link the undeformed geometry across faults.

Figure 3(a) is an extensional structure from off-shore Nigeria, Fig. 3(b) is a restoration using affine transformations and Fig. 3(c) a restoration using non-linear transformations.

In Fig. 3(b) gaps and overlaps between adjacent fault blocks are minimized by using a combination of rigid rotation, translation and simple shear. Note that the fault on the left-hand side of Fig. 3(a) is artificial: there is no displacement on it and it merely serves to divide the cross-section into blocks that can have different geometric transformations. The solid black and white areas in Fig. 3(b) are overlaps and gaps, respectively, between fault blocks which exist because an affine transformation (simple shear) was used. If the gaps and overlaps are minimized, then the artificial fault on the left-hand side of the restored section (Fig. 3b) now has offset which is an artifact of the transformation algorithm. In the same way, the offset on the other fault is probably in error because of the limitations of affine transformations. These errors may not be too significant if the user is only interested in balancing: making a geometric check on the interpretation. However, if one is interested in relating paleostructure to generation and migration of hydrocarbons, paleo-offset on faults can be critical.

Figure 3(c) is a non-linear restoration. Note that the artificial fault has no displacement in the restored section, there are no gaps or overlaps, the offset on the 'real' fault is quite different compared to Fig. 3(b), and the loose line on the left-hand side of the restoration correctly shows that the lower layers have less line length than the upper ones in this growth fault environment.

Figure 4(a) is a compressional structure from Peru based on outcrop and seismic data. There are significant thickness changes in the upper two units, especially in the anticline.

Figure 4(b) is a linear restoration based on layer-

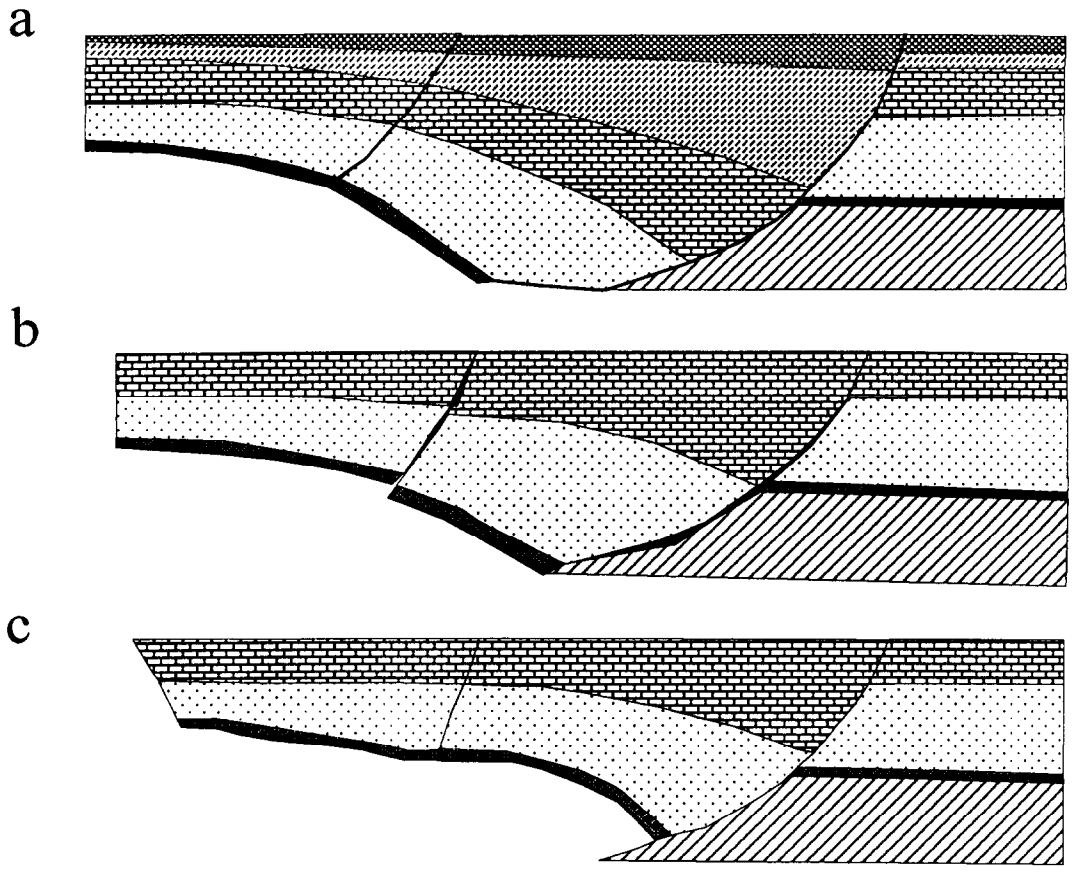

Fig. 3. (a) A cross-section interpreted from a seismic line off-shore Nigeria depicting a listric normal fault with growth and roll-over on the hanging wall. Note the fault on the left is purely artificial: it has no displacement and serves only to divide the cross-section into three regions. (b) Cross-section in (a) restored using inclined simple shear, rigid rotation and translation in the three regions separated by faults. The simple-shear angle and rotation and translation were adjusted to qualitatively minimize gaps and overlaps between the three regions. Gaps and overlaps are represented by white and black areas, respectively. Note the left fault has offset in the restored section which is an artifact of the linear simple-shear transformation used in the restoration. (c) Cross-section in (a) restored using non-linear transformation equations. Note the left fault can be restored without offset; the loose line on the left-hand side of the restored section accurately shows less line length in the lower strata.

parallel simple shear. Each layer in the cross-section (Fig. 4a) was divided into quadrilateral domains which were then successively restored from left to right. Because the affine transformation is over-constrained, the domains cannot be fitted together, and gaps (blank areas) and overlaps (black areas) are especially prominent where thickness changes occur. In addition, the same boundary between two layers may have different lengths (see the loose-line on the right-hand side of Fig. 4b). This also produces gaps and overlaps along the fault on the right side of the restoration (Fig. 4b).

In Fig. 4(c)–(e) all restorations use a non-linear transformation and a quadrilateral mesh. Because each quadrilateral has a thickness associated with it, the user can control the thickness in the undeformed restoration and generate a variety of paleostructures depending on the assumptions. In Fig. 4(c) it is assumed that the variable thickness in the cross-section (Fig. 4a) is due to tectonic strain and not due to original depositional thickness. The thickness in the restored section (Fig. 4c) is constant in each layer in each fault block.

Alternatively, in Fig. 4(d), it is assumed that the initial thickness varied linearly in each fault block. Note that the paleostructure in Fig. 4(d) is quite different compared to Fig. 4(c). In Fig. 4(d) there is almost no displacement on the left fault which is near the crest of a gentle anticline. The right-hand side fault is a paleogrowth fault which has been inverted to generate the modern structure (Fig. 4a)

Figure 4(e) assumes that the modern thickness was also the initial thickness. This implies that the anticline in Fig. 4(a) is an inverted basin and the left-hand side fault was a reverse fault which was active during sedimentation.

These three possible paleostructures have very different tectonic implications and could have important economic differences when the timing of hydrocarbon generation and migration is considered. The choice is an informed judgment of the geologist. For example, Fig. 4(e) (ancient and modern thickness are the same) is least likely. It does not 'balance' well, and the conversion of a syncline into an anticline by layer-parallel compression is mechanically unlikely. Unless regional stratigraphic and tectonic data preclude it, Fig. 4(d) seems most likely.

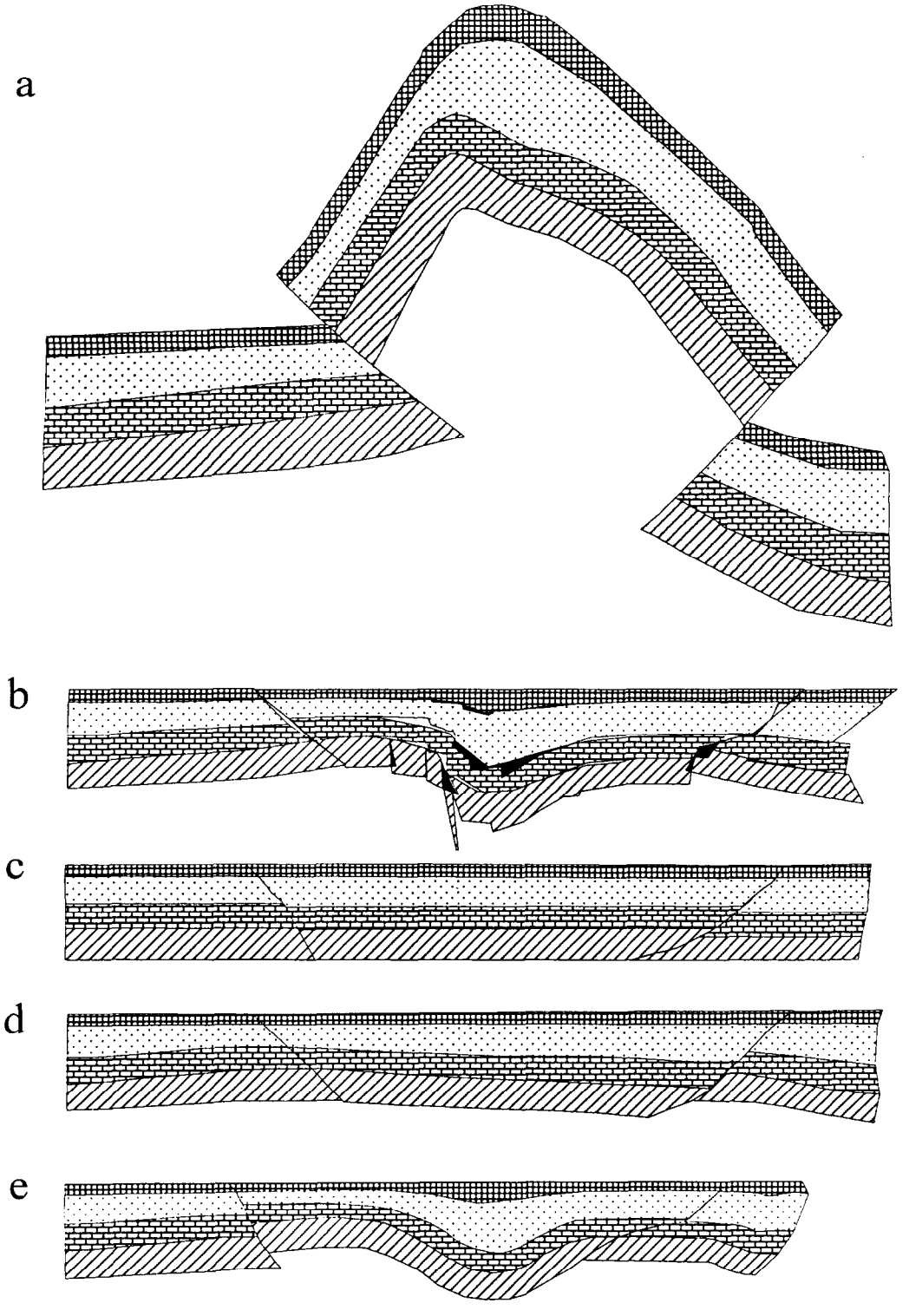

Fig. 4. (a) A cross-section interpreted from a seismic line from Peru. Note thickness changes in upper strata. (b) The cross-section of (a) restored using layer-parallel simple shear. The gaps and overlaps are shown by white and black areas, respectively, and are the result of using layer-parallel simple shear where there are thickness changes. Note also that line lengths on the same layer boundary differ depending on whether measured as the bottom of the overlying layer or the top of the underlying layer (see the loose-line on the right-hand side of the restored section). (c) A restored section using quadrilateral domains and non-linear transformations. It was assumed that initial layer thicknesses were constant in each fault block. This restoration suggests that the right fault was a reverse growth fault while the left fault was normal. (d) A restored section using quadrilateral domains and non-linear transformations. It was assumed that initial layer thickness varied linearly in each fault block. This restoration suggests that the right-hand side fault was a normal growth fault, and the left-hand side fault was not active but was the site of a paleo-anticline. (e) A restored section using quadrilateral domains and non-linear transformations. It was assumed that initial layer thickness was the same as presently occurs in the modern structure (a). This produces a paleo-syncline at the site of the modern anticline. The left fault is now reverse, while the right fault has almost no displacement.

CONCLUSIONS

(1) Affine transformations such as simple shear, pure shear, rigid rotation and translation, or any combination of these special cases, cannot preserve both area and continuity of adjacent regions and, in general, should not be used to restore cross-sections and infer paleostructure.

(2) Continuity and area can be preserved using non-linear transformations and quadrilateral domains. Dividing the cross-section into quadrilateral domains also provides control of thickness changes and gives more flexibility and detail to the restoration.

(3) If non-linear analytical equations are used to transform quadrilaterals from the deformed to the undeformed state, the finite-strain distribution can be calculated at any point in the cross-section.

(4) If finite strain can be measured in the rocks, these data can be included in the restoration process to provide an important additional constraint on the reliability of the restoration.

REFERENCES

Biot, M. A. (1965) *Mechanics of Incremental Deformations*. John Wiley and Sons, New York.

Bucher, W. H. (1933) *The Deformation of the Earth's Crust*. Princeton University Press, Princeton, New Jersey.

Butler, R. W. H. (1983) The restoration of thrust systems and displacement continuity around the Mont Blank massif, NW external Alpine thrust belt. *Journal of Structural Geology* **5**, 569–582.

Chamberlain, R. T. (1910) The Appalachian folds of Central Pennsylvania. *Journal of Geology* **18**, 228–251.

Cobbold, P. R. (1979) Removal of finite deformation using strain trajectories. *Journal of Structural Geology* **1**, 67–72.

Cobbold, P. R. and Percevault, M.-N. (1983) Spatial integration of strains using finite elements. *Journal of Structural Geology* **5**, 299–305.

Colletta, B., Hebrard, F., Letouzey, J., Werner, P. and Rudkiewicz, J. L. (1990) Tectonic style and crustal structure of the eastern cordillera (Columbia) from a balanced cross section. In *Petroleum and Tectonics in Mobile Belts*, ed. J. Letouzey, pp. 81–100. Éditions Technip, Paris.

Cook, D. G. (1988) Balancing basement-cored folds of the Rocky Mountain foreland. *Geological Society of America Memoir* **171**, 53–64.

Cooper, M. A. (1983) The calculation of bulk strain in oblique and inclined balanced sections. *Journal of Structural Geology* **5**, 161–165.

Cooper, M. A. and Trayner, P. M. (1986) Thrust surface geometry: implications for thrust-belt evolution and section-balancing techniques. *Journal of Structural Geology* **8**, 305–312.

Dahlstrom, C. D. A. (1969) Balanced cross sections. *Canadian Journal of Earth Sciences* **6**, 743–757.

De Paor, D. G. (1987) Stretch in shear zones: implications for section balancing. *Journal of Structural Geology* **9**, 893–895.

De Paor, D. G. (1990) Cross-section balancing in space and time. In *Petroleum and Tectonics in Mobil Belts*, ed. J. Letouzey, pp. 149–154. éditions Technip, Paris.

DePaor, D. G. and Bradley, D. C. (1988) Balanced sections in thrust belts, Part 2: computerized line and area balancing. *Geobyte* **3**(5), 33–37.

Elliott, D. (1983) The construction of balanced cross sections. *Journal of Structural Geology* **5**, 101.

Endignoux, L. and Mugnier, J.-L. (1990) The use of a forward kinematic model in the construction of balanced cross-sections. *Tectonics* **9**, 1249–1262.

Erslev, E. A. (1986) Basement balancing of Rocky Mountain foreland uplifts. *Geology* **14**, 259–262.

Espina, R. G., Alonso, J. L. and Pulgar, J. A. (1996) Growth and propagation of buckle folds determined from syntectonic sediments (the Ubierna Fold Belt Cantabrian Mountains, N. Spain). *Journal of Structural Geology* **18**, 431–441.

Ford, M. (1987) Practical application of the sequential balancing technique: an example from the Irish Variscides. *Journal of the Geological Society of London* **144**, 885–891.

Freeth, S. J. and Ladipo, K. O. (1986) The development and restoration of syn-sedimentary faults. *Earth and Planetary Science Letters* **78**, 411–419.

Geiser, J., Geiser, P. A., Kligfield, R., Ratliff, R. and Rowan, M. (1988) New applications of computer-based section construction: strain analysis, local balancing, and subsurface fault prediction. *Mountain Geologist* **25**(2), 47–59.

Geiser, P. A. (1988) The role of kinematics in the construction and analysis of geological cross-sections in deformed terranes. In *Geometrics and Mechanisms of Thrusting*, eds G. Mitra and S. Wojtal, pp. 47–76. Geological Society of America Special Paper **222**.

Gibbs, A. D. (1983) Balanced cross-section construction from seismic sections in areas of extensional tectonics. *Journal of Structural Geology* **5**, 153–160.

Gougel, J. (1962) *Tectonics*. W. H. Freeman, San Francisco.

Gratier, J.-P., Guillier, B. and Delorme, A. (1991) Restoration and balance of a folded and faulted surface by best-fitting of finite elements: principle and applications. *Journal of Structural Geology* **13**, 111–115.

Guillier, B. and Gratier, J.-P. (1991) Dépliage automatique de surfaces: tests de la géométrie des strates plissées. *Comptes rendus de l'Académie des Sciences, Paris* **313**, 1313–1318.

Hossack, J. R. (1978) The correction of stratigraphic sections for tectonic finite strain in the Bygdin area, Norway. *Journal of the Geological Society of London* **135**, 229–241.

Hossack, J. R. (1979) The use of balanced cross-sections in the calculations of orogenic contractions. *Journal of the Geological Society of London* **136**, 705–711.

Howard, J. H. (1993) Restoration of cross-sections through unfaulted, variably strained strata. *Journal of Structural Geology* **15**, 1331–1342.

Julivert, M. and Arboleya, M. L. (1986) Area balancing and estimate of areal reduction in a thin-skinned fold-and-thrust belt (Cantabrian zone, NW Spain): constraints on its emplacement mechanism. *Journal of Structural Geology* **8**, 407–414.

Kligfield, R. P., Geiser, P. and Geriser, J. (1986) Construction of geologic cross-sections using microcomputer systems. *Geobyte* **1**, 60–66.

Lisle, R. J. (1992) Constant bed-length folding: three-dimensional geometrical implications. *Journal of Structural Geology* **14**, 245–252.

McCoss, A. M. (1988) Restoration of transpression/transtension by generating the three-dimensional segmented helical loci of deformed lines across structure contour maps. *Journal of Structural Geology* **10**, 109–120.

McDougall, J. W. and Hussain, A. (1991) Fold and thrust propagation in the Western Himalaya based on a balanced cross-section of the Surghar Range and Kohat Plateau, Pakistan. *Bulletin of the American Association of Petroleum Geologists* **75**, 463–478.

Means, W. D. (1976) *Stress and Strain*. Springer, New York.

Mitra, S. and Namson, J. (1989) Equal-area balancing. *American Journal of Science* **289**, 563–599.

Moretti, I. and Larrére, M. (1989) LOCACE: Computer-aided construction of balanced geological cross-sections. *Geobyte* **4**(5), 16–24.

Moretti, I., Triboulet, S. and Endignoux, L. (1990) Some remarks on the geometrical modeling of geological deformations. In *Petroleum and Tectonics in Mobile Belts*, ed. J. Letouzey, pp. 155–162. Éditions Technip, Paris.

Morgan, J. K. and Karig, D. E. (1995) Kinematics and a balanced and restored cross-section across the toe of the eastern Nankai accretionary prism. *Journal of Structural Geology* **17**, 31–45.

Morgan, J. K., Karig, D. E. and Maniatty, A. (1994) The estimation of diffuse strains in the toe of the western Nankai accretionary prism: A kinematic approach. *Journal of Geophysical Research* **99**, 7019–7032.

Mount, V. S., Suppe, J. and Hook, S. C. (1990) A forward modeling strategy for balancing cross-sections. *Bulletin of the American Association of Petroleum Geologists* **74**, 521–531.

Mugnier, J.-L. and Rosetti, J. P. (1990) The effects of simplifying assumptions on balanced cross-sections: a view from the Chartreuse Massif. In *Petroleum and Tectonics in Mobile Belts*, ed. J. Letouzey, pp. 167–180. Éditions Technip, Paris.

Nunns, A. G. (1991) Structural restoration of seismic and geologic sections in extensional regimes. *Bulletin of the American Association of Petroleum Geologists* **75**, 278–297.
Oertel, G. (1974) Unfolding of an antiform by the reversal of observed strains. *Bulletin of the Geological Society of America* **85**, 445–450.
Oertel, G. and Ernst, W. G. (1978) Strain and rotation in a multilayered fold. *Tectonophysics* **48**, 77–106.
Protzman, G. M. and Mitra, G. (1990) Strain fabric associated with the Meade thrust sheet: implications for cross-section balancing. *Journal of Structural Geology* **12**, 403–417.
Ramsay, J. G. and Huber, M. I. (1983) *Techniques of Modern Structural Geology*, Vol. 1. Academic Press, New York.
Rowan, M. G. and Kligfield, R. (1989) Cross-section restoration and balancing as an aid to seismic interpretation in extensional terranes. *Bulletin of the American Association of Petroleum Geologists* **73**, 955–966.
Sage, L., Mosconi, A., Moretti, I., Riva, E. and Roure, F. (1991) Cross-section balancing in the Central Apennines: an application of LOCACE. *Bulletin of the American Association of Petroleum Geologists* **75**, 832–844.
Schneider, C. L., Hummon, C., Yeats, R. S. and Huftile, G. L. (1996) Structural evolution of the northern Los Angeles basin, California, based on growth strata. *Tectonics* **15**, 341–355.
Schwerdtner, W. M. (1977) Geometric interpretation of regional strain analysis. *Tectonophysics* **39**, 515–531.
Searle, M. P., Pickering, K. R. and Cooper, D. J. W. (1990) Restoration and evolution of the intermontane Indus molasse basin, Ladakh Himalaya, India. *Tectonophysics* **174**, 301–314.
Suppe, J. (1983) Geometry and kinematics of fault-bend folding. *American Journal of Science* **283**, 684–721.
Townsend, C. (1987) Thrust transport directions and thrust sheet restoration in the Caledonides of Finnmark, North Norway. *Journal of Structural Geology* **9**, 345–352.
Triboulet, S. (1990) Balanced cross-section with anisopachous layers using LOCACE software. In *Petroleum and Tectonics in Mobile Belts*, ed. J. Letouzey, pp. 163–166. Éditions Technip, Paris.
Williams, G. D. (1984) The calculation of horizontal thrust transport using excess area in cross-sections. *Tectonophysics* **104**, 177–182.
Williams, G. D. and Brooks, M. (1985) A reinterpretation of the concealed Variscan structure beneath southern England by section balancing. *Journal of the Geological Society of London* **142**, 689–695.
Woodward, N. B., Gray, D. R. and Spears, D. B. (1986) Including strain data in balanced cross-sections. *Journal of Structural Geology* **8**, 313–324.

APPENDIX I

Constraints across faults

Constraints on deformation at fault boundaries can be derived from geometrical consequences of continuity, and non-linear analysis is essential to establish required boundary conditions at faults. In the deformed configuration (the cross-section), let: $x_i = \hat{x}_i(s)$ represent the fault curve λ with arc length s along the curve λ. In the deformed configuration, we can regard the curve as separating two material regions r^- and r^+. Motions $X_i^-(x_j^-)$ and $X_i^+(x_j^+)$ transform particles in regions r^- and r^+ in the deformed state to regions R^- and R^+ in the undeformed state whose common boundary is the undeformed fault curve Λ. In order to establish the position of a fault in the undeformed configuration, the curve $\Lambda : X_i = X_i^-[\hat{x}_j(s)]$ is determined by extrapolation with the cross-section restoration algorithm in the region r^- in the limit as particles in r^- approach the fault curve λ. We suppose the motion sufficiently smooth to compute

$$dX_i^- = (\partial X_i^-/\partial x_j^-) l_j ds, \tag{A1}$$

where $l_j = d\hat{x}_i/ds$ is the unit tangent vector to the curve λ.

An element of arc length S^- on the undeformed fault can be computed from

$$(dS^-)^2 = dX_i^- dX_i^- = c_{ij}^- l_i l_j (ds)^2, \tag{A2}$$

where c_{ij}^- is the right Cauchy–Green strain tensor. Because the Cauchy–Green tensor is always positive definite,

$$dS^-/ds > 0, \tag{A3}$$

and the arc length function $S^- = S^-(s)$ is invertable so as to allow the construction of the inverse function $s = s^-(S^-)$. Thus there is a one-to-one correspondence of points on the fault curves λ and Λ.

Particles in the regions r^- and r^+ adjacent to the point s on the deformed fault curve λ will not generally remain adjacent to a point S on the undeformed curve Λ. The motions $X_i^-(x_j^-)$ and $X_i^+(x_j^+)$ produce finite deformations that can induce large motions along a fault. It follows that particles $X_i^-[\hat{x}_j(s)]$ and $X_i^+[\hat{x}_j(s)]$ on the undeformed fault Λ can be separated by a large distance.

In order to analyze continuity conditions required along the undeformed fault curve Λ, we introduce the fault motion function $s_f(s)$. The fault motion function provides a correspondence on the curve λ for points mapped from the regions r^- and r^+ with the motions $X_i^-(x_j^-)$ and $X_i^+(x_j^+)$, respectively, at the common boundary λ for points on the curve Λ, the common boundary of regions R^- and R^+ in the undeformed configuration. Analogous to equations (A1) and (A2) above, we suppose the motion $X_i^+(x_j^+)$ sufficiently smooth to compute

$$dX_i^+ = \partial X_i^+/\partial x_j^+ l_j ds \tag{A4}$$

and

$$(dS^+)^2 = dX_i^+ dX_i^+ = c_{ij}^+ l_i l_j (ds)^2. \tag{A5}$$

Equation (A5) provides a means to calculate arc length S^+ on Λ from the motion $X_i^+(x_j^+)$and the representation $\hat{x}_j(s)$ for the fault curve λ in the deformed configuration. The fault motion function is defined by

$$S^-(s) = S = S^+[s_f(s)]. \tag{A6}$$

In words, the fault motion function maps points of the line λ onto itself such that preferred particles on opposite sides of the fault λ will transform to the same point S on the undeformed fault curve Λ from the motion X_i^- and X_i^+. The common measure of arc length on the undeformed fault Λ is denoted by S. For material continuity, $ds_f/ds > 0$, and the fault displacement can be defined by $u_f(s) = s_f(s) - s$.

With the fault motion function, we can state our assumption about continuity along the undeformed fault curve Λ. The continuity conditions are:

$$X_i^-[x_j(s)] = X_i^+[x_j(s_f)] \text{ on } \Lambda. \tag{A7}$$

This condition assures that the motions X_i^- and X_i^+ deliver particles on the fault with no opening or overlap. This condition may be written

$$X_i = \overset{\wedge}{(X_i^- - X_i^+)} = 0. \tag{A8}$$

Discontinuities of X_i are spread out smoothly over Λ so that, in particular,

$$dX_i/dS = 0 \text{ on } \Lambda. \tag{A9}$$

The smoothness requirements stated in equations (A8) and (A9) provide restrictions on the motions X_i^- and X_i^+ along the fault Λ.

Unit tangent vectors L_i^- and L_i^+ at a point S of L derived from the motion X_i^- and X_i^+, respectively, must be equal, that is with

$$L_i^- = dX_i^-(s)/dS = \partial X_i^-/\partial x_k^- 1_k(s)(ds/dS) \tag{A10}$$

and

$$L_i^+ = \partial X_i^+(s_f)/\partial x_k^+ 1_k(s_f)\, ds_f/ds\, ds/dS. \tag{A11}$$

Then geometrical compatibility ($L_i^- = L_i^+$ on Λ) requires

$$\partial X_i^-(s)/\partial x_k^- 1_k(s) = \partial X_i^+(s_f)/\partial x_k^+ 1_k(s_f)\, ds_f/ds. \tag{A12}$$

The relationship provided in equation (A12) together with the identity

$$\delta_{ik} = 1_i(s_f)1_k(s_f) + n_i(s_f)n_k(s_f), \tag{A13}$$

where δ_{ik} is the 2×2 unit matrix and $n_i(s_f)$ is a unit normal vector to the deformed fault λ at the point s_f, allow the representation

$$\begin{aligned}\partial X_i^+(s_f)/\partial x_j^+ = &[\partial X_i^+(s_f)/\partial x_k^+ n_k(s_f)]n_j(s_f) \\ &+ [\partial X_i^-/\partial x_k^- 1_k(s)]1_j(s_f)/(ds_f/ds).\end{aligned} \tag{A14}$$

Equation (A14) gives a representation of the unknown deformation gradient D_{ij}^{+} on λ in terms of known tangential components of D^{-} and unknown normal components of the deformation gradients D^{+}. Our smoothness assumptions allow further differentiation of equations (A10) and (A11) along the fault curve Λ. Let $N_i(S)$ denote the unit normal vector to the curve Λ. Application of the Frenét formula

$$dL_i/dS = K_\Lambda N_i, \tag{A15}$$

where K_Λ is the curvature of the fault Λ, and computation of the derivatives dL_i^{-}/dS and dL_i^{+}/ds provides the formulae

$$\begin{aligned} K_\Lambda^{-} N_i^{-} =& \partial^2 X_i^{-}(s)/\partial x_j^{-}\partial x_k^{-} l_j(s) l_k(s)(ds/dS)^2 \\ &+ \partial X_i^{-}(s)/\partial x_j^{-} n_j(s)\kappa_\lambda(s)(ds/dS)^2 \\ &+ \partial X_i^{-}(s)/\partial x_j^{-} l_j(s)(d^2 s/dS^2) \end{aligned} \tag{A16}$$

$$\begin{aligned} K_\Lambda^{+} N_i^{+} =& \partial^2 X_i^{+}(s_f)/\partial x_j^{+}\partial x_k^{+} l_j(s_f) l_k(s_f)(ds_f/ds)^2(ds/dS)^2 \\ &+ \partial X_i^{+}(s_f)/\partial x_j^{+} n_j(s_f)\kappa_\lambda(s_f)(ds_f/ds)^2(ds/dS)^2 \\ &+ \partial X_i^{+}(s_f)/\partial x_j^{+} l_j(s_f) q(S), \end{aligned} \tag{A17}$$

where

$$q(S) = d^2 s_f/ds^2(ds/dS)^2 + (ds_f/ds)(d^2 s/dS^2) \tag{A18}$$

and κ_λ is the curvature of the deformed fault curve λ.

Geometric compatibility requires that $K_\Lambda^{-} = K_\Lambda^{+}$ and $N_i^{-}(S) = N_i^{+}(S)$. All of the compatibility relationships of equations (A10), (A11), (A16) and (A17) can be used to constrain the state of deformation in the region R^{+} along the undeformed fault Λ when representations for the motions X_i^{-} and X_i^{+} in the neighborhood of a fault are supplied.

In the case that either (a) the deformations D^{-} and D^{+} are homogeneous (linear) or (b) the vectors $v_i^{-} = \partial^2 X_i^{-}(s)/\partial x_j^{-}\partial x_k^{-} l_j(s) l_k(s)$ and $v_i^{+} = \partial^2 X_i^{+}(s_f)/\partial x_j^{+}\partial x_k^{+} l_j(s_f) l_k(s_f)$ appearing in equations (A16) and (A17) are negligibly small, we can calculate the state of deformation $\partial X_i^{+}(s_f)/\partial x_j^{+}$ in the region R^{+} on the fault Λ without recourse to specific forms of the motion X_i^{-} and X_i^{+} along a fault. Equations (A14) and (A17) provide the estimate

$$\begin{aligned} \partial X_i^{+}(s_f)/\partial x_j^{+} n_j(s_f) =& [K_\Lambda^{+}(ds_f/ds) N_i^{+}(S) \\ &- \partial X_i^{-}(s)/\partial x_j^{-} l_j(s) q(S)]/[\kappa_\lambda(s_f)(ds_f/ds)^3(ds/dS)^2]. \end{aligned} \tag{A19}$$

Substitution of the result of equation (A19) into equation (A14) provides the result

$$\begin{aligned} \partial X_i^{+}(s_f)/\partial x_j^{+} =& [K_\Lambda(ds_f/ds) N_i(S) \\ &- \partial X_i^{-}(s)/\partial x_k^{-} l_k(s) q(S)] n_j(s_f)/[\kappa_\lambda(s_f)(ds_f/ds)^3(ds/dS)^2] \\ &+ \partial X_i^{-}(s)/\partial x_k^{-} l_k(s) l_j(s_f)/(ds_f/ds). \end{aligned} \tag{A20}$$

This last formulae provides an estimate of D_{ij}^{+} in the region R^{+} along the fault when the deformation D_{ij}^{-}, the fault curvatures K_Λ and κ_λ, the unit tangent and normal vectors l_j, n_i and N_i on the deformed and undeformed faults respectively, the fault length function $S = S(s)$, and the fault motion functions $s_f(s)$ are prescribed or calculated in restoration computations.

Use of equations (A19) and (A20) will be inappropriate when the fault curve λ in the deformed configuration is a straight line ($\kappa_\lambda = 0$). When the motions X_i^{-} and X_i^{+} are homogeneous or the vectors vi^{-} and v_i^{+} vanish, then the computation of the inner products of equations (A16) and (A17) with the unit tangent vector L_i and unit normal vector N_i of the undeformed fault Λ shows that

$$(d^2 s/dS^2) = 0;\ q(S) = 0;\ \text{and}\ K_\Lambda = 0. \tag{A21}$$

These results imply that: (i) the undeformed fault curve Λ must also be a straight line; (ii) the deformed and undeformed fault curves λ and Λ are related by a uniform stretch $s = \sigma S + \sigma_0$, where σ and σ_0 are constants; and (iii) the fault motion function $s_f(s)$ is the linear function $s_f(s) = \alpha s + \beta$, with α and β constant. In this simple class of deformations, a fault can still be stretched, rotated and translated. In general, it is unreasonable to assume that a straight line fault in the deformed configuration cannot be transformed into a curved fault in the undeformed configuration. Here again we affirm the necessity to work with inhomogeneous (non-linear) transformations in section restoration.

In our practice of two-dimensional restoration, we employ the geometric compatibility condition, equation (A12), in the form

$$c_{ij}^{-} l_i l_j|_{s_i^{-}} = c_{ij}^{+} l_i l_j (ds_f/ds)^2|_{s_i^{-}}, \tag{A22}$$

where s_i^{-} and s_i^{+} refer to formation units in regions r^{-} and r^{+} adjacent to a fault. This means that thicknesses for such a unit along the faults Λ and λ are related according to the ratio

$$\Delta S^{-}/\Delta s^{-} = \Delta S^{+}/\Delta s^{+}. \tag{A23}$$